THE JOURNAL OF BIOLOGICAL CHEMISTRY VOL. 291, NO. 25, pp. 13113–13123, June 17, 2016

A Functional Study of Mutations in K^+-dependent Na^+-Ca^{2+} Exchangers Associated with Amelogenesis Imperfecta and Non-syndromic Oculocutaneous Albinism*

Received for publication, March 22, 2016, and in revised form, April 15, 2016 Published, JBC Papers in Press, April 25, 2016, DOI 10.1074/jbc.M116.728824

Ali H. Jalloul, Tatiana P. Rogasevskaia, Robert T. Szerencsei, and Paul P. M. Schnetkamp[1]

From the Department of Physiology and Pharmacology, Hotchkiss Brain Institute, Cumming School of Medicine, University of Calgary, Calgary, Alberta T2N 4N1, Canada

K^+-dependent Na^+/Ca^{2+} exchangers belong to the solute carrier 24 (*SLC24A1–5*) gene family of membrane transporters. Five different gene products (NCKX1–5) have been identified in humans, which play key roles in biological processes including vision, olfaction, and skin pigmentation. NCKXs are bi-directional membrane transporters that transport 1 Ca^{2+}+K^+ ions in exchange for 4 Na^+ ions. Recent studies have linked mutations in the *SLC24A4* (NCKX4) and *SLC24A5* (NCKX5) genes to amelogenesis imperfecta (AI) and non-syndromic oculocutaneous albinism (OCA6), respectively. Here, we introduced mutations found in patients with AI and OCA6 into human *SLC24A4* (NCKX4) cDNA leading to single residue substitutions in the mutant NCKX4 proteins. We measured NCKX-mediated Ca^{2+} transport activity of WT and mutant NCKX4 proteins expressed in HEK293 cells. Three mutant NCKX4 cDNAs represent mutations found in the *SCL24A4* gene and three represent mutations found in the *SCL24A5* gene involving residues conserved between NCKX4 and NCKX5. Five mutant proteins had no observable NCKX activity, whereas one mutation resulted in a 78% reduction in transport activity. Total protein expression and trafficking to the plasma membrane (the latter with one exception) were not affected in the HEK293 cell expression system. We also analyzed two mutations in a *Drosophila* NCKX gene that have been reported to result in an increased susceptibility for seizures, and found that both resulted in mutant proteins with significantly reduced but observable NCKX activity. The data presented here support the genetic analyses that mutations in *SLC24A4* and *SLC24A5* are responsible for the phenotypic defects observed in human patients.

Calcium (Ca^{2+}) transport is essential for the mineralization of hard tissues such as bone and enamel (1). It is well recognized that a Ca^{2+} flux exists across the ameloblast epithelium to form the bone mineral hydroxyapatite; most of this flux is believed to follow the transcellular route rather than the paracellular route, which entails a role for Ca^{2+} channels to provide passage for Ca^{2+} entry (2). There is evidence for two different Ca^{2+} channels that are important for Ca^{2+} entry into the ameloblasts: the L-type voltage-gated Ca_v1 channel localized on the plasma membrane and the store-operated Ca^{2+} channel. Mutations in the *CACNA1C* gene that codes for the Ca_v1 channel are associated with Timothy syndrome, which is a multisystem disorder presented with enamel hypoplasia, small teeth, and several other physiological abnormalities in the heart and other organs (OMIM 601005) (3). Stim1 proteins, located in the endoplasmic reticulum, are activated by the depletion of endoplasmic reticulum Ca^{2+} and induce Ca^{2+} influx into the cell by the activation of the ORAI1 store-operated plasma membrane channel. Recently, enamel defects were reported for patients with mutations in the *STIM1* gene (NM_001277961.1) (4, 5). In addition, transcripts of the *STIM1* gene were abundantly expressed during the maturation stage (4, 6). The involvement of ORAI/STIM1 channels suggested a new paradigm of Ca^{2+} transport involving an organellar pathway for the transport of endoplasmic reticulum-stored Ca^{2+} across the enamel epithelium instead of transcytosis. Such a pathway would allow ameloblasts to supply large amounts of Ca^{2+} while avoiding the cytotoxic effects of high levels of intracellular free Ca^{2+} (6).

Efficient basal Ca^{2+} entry requires efficient apical Ca^{2+} extrusion to the developing enamel and this is now thought to be mediated by Na^+/Ca^{2+} exchangers. Na^+/Ca^{2+} exchangers belong to either the *SLC8A*[2] gene family of K^+-independent Na^+/Ca^{2+} exchangers, encoding three distinct NCX1–3 proteins (7), or the *SLC24A* gene family of K^+-dependent Na^+/Ca^{2+} exchangers encoding the five distinct NCKX1–5 proteins (8). Transcripts of both NCXs and NCKXs were expressed at different stages of the developing enamel (9, 10), specifically NCX1, NCX3, and NCKX4. Moreover, the highest *SLC24A4* gene (accession number AF520705) transcript levels were observed in maturation-stage ameloblasts and the NCKX4 protein was localized at the apical pole suggesting that NCKX4 is a key Ca^{2+} transporter during amelogenesis (10). The importance of the *SLC24A4* gene is corroborated by recent genetic analyses linking three unique *SLC24A4* missense mutations to amelogenesis imperfecta (AI) (4, 11–13), a genetic disease presented with abnormal teeth formation and development. *Slc24a4*$^{-/-}$ mice displayed enamel malformations and defects similar to those seen in human patients with AI (12), which provides further support for the important role of NCKX4 pro-

* This work was supported by Canadian Institutes for Health Research operating Grant MOP-81327. The authors declare that they have no competing financial interests.

[1] To whom correspondence should be addressed: 3230 Hospital Dr. NW, Calgary, Alberta T2N 4N1, Canada. Tel.: 403-220-6862; E-mail: pschnetk@ucalgary.ca.

[2] The abbreviations used are: *SLC*, solute carrier gene family; AI, amelogenesis imperfecta; NCKX, K^+-dependent Na^+-Ca^{2+} exchangers; NCX, Na^+-Ca^{2+} exchangers; TMS, transmembrane segment; OCA6, oculocutaneous albinism.

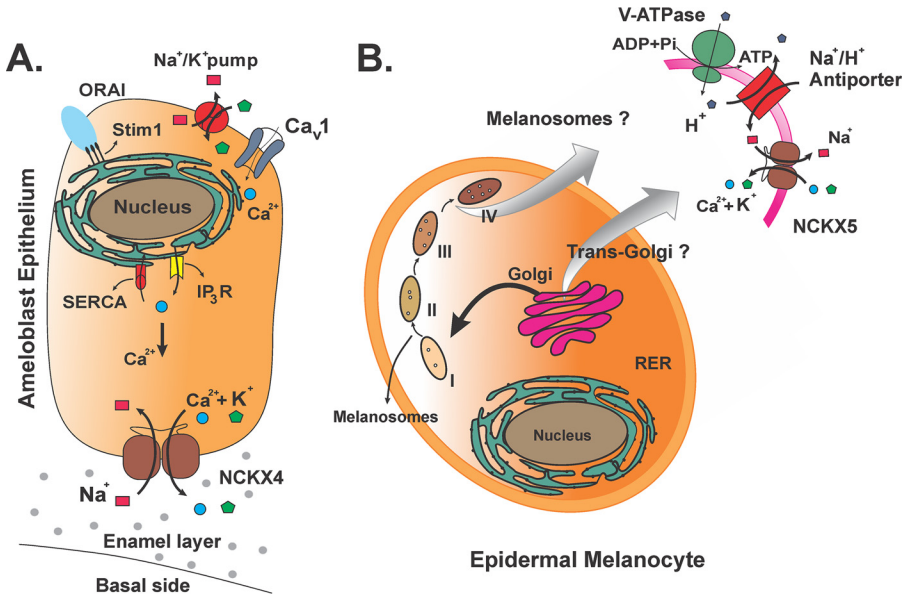

FIGURE 1. **Physiological settings for NCKX4 function in ameloblast cells and NCKX5 function in epidermal melanocytes cells.** *A,* NCKX4 role in Ca^{2+} signaling of ameloblasts: as discussed in the text, apical Ca^{2+} entry into the ameloblast cytoplasm may be mediated by L-type voltage-gated channels (Ca_V1) or store-operated Ca^{2+} channels (*ORAI*). Next, Ca^{2+} may be stored in the endoplasmic reticulum for later release by activating inositol 3-phosphate receptors (*IP_3R*), and, finally, basolateral release of Ca^{2+} into the enamel layer is mediated by NCKX4 where it contributes to the formation of mineral hydroxyapatite crystals. Furthermore, the Na^+ and K^+ gradients used by NCKX4 to extrude Ca^{2+} are restored via the Na^+/K^+-ATPase. *B,* proposed role of NCKX5 in epidermal melanocytes. As NCKX5 is not located in the cell surface membrane, the first study to report on the role of NCKX5 in pigmentation proposed a role for NCKX5 in neutralizing the pH in melanosomes, which are derived from acidic organelles (18). The V-ATPase proton pump maintains an acidic environment inside the organelles, which can then be neutralized via an organellar Na^+/H^+ antiporter. As the Na^+ concentration in the organelle increases, NCKX5 is proposed to lower organellar Na^+ by coupled transport with Ca^{2+} and K^+ from the cytoplasm. Subsequent studies have reported that NCKX5 is located in late stage melanosomes (26) or in the Trans-Golgi network (27), and the above model could apply to both. To date, NCKX5-mediated Ca^{2+} transport has yet to be demonstrated in epidermal melanocytes.

teins in tooth development. NCKX4 appears to play important roles in other tissues; for instance, *Slc24a4*$^{-/-}$ mice also have olfactory deficits (14) and display changes in melanocortin-4-receptor-dependent signaling that leads to satiety (15). Finally, association studies have suggested a role for the *SLC24A4* gene in variations in hair and eye pigmentation in European populations (16, 17).

Another member of the NCKX family, the *SLC24A5* gene has been shown to be the major genetic determinant of light skin in people from European descent (18, 19), and three distinct *SLC24A5* mutations have been linked to oculocutaneous albinism (OCA6) (20, 21). Fig. 1 illustrates physiological models for NCKX4 and NCKX5 function in ameloblasts and skin cells, respectively. In addition to studies describing NCKX mutations in human patients, two single residue substitutions in the *Drosophila Nckx-x* (*Zydeco*) gene have been associated with an increased susceptibility to seizures (22); *Nckx-x* is most closely related to the *SLC24A3 and SLC24A4* compared with the other three *SLC24* genes.

Relatively little has been reported on the functional and structural properties of the NCKX4, NCKX5, and NCKX-X proteins unlike the extensive functional and structural studies on NCKX1 and NCKX2 (23). NCKX4 and NCKX-X are trafficked to the plasma membrane and operate there as K^+-dependent Na^+/Ca^{2+} exchangers (24, 25). In contrast, the NCKX5 protein is not found in the plasma membrane but has been reported to be localized in the melanosomal membranes (26) or the Trans-Golgi network (27). Given the high degree of sequence identity in the transmembrane segments (TMS) between NCKX1–5 and the high degree of similarity in the kinetic parameters between NCKX1–4 (28) it is reasonable to suggest that NCKX1–5 share the same topology reported for NCKX2 (29, 30) and the same transport stoichiometry (4 $Na^+ \leftrightarrow$ 1 Ca^{2+} and 1 K^+) reported for NCKX1 and NCKX2 (31–33). Here we present the functional consequences of mutations in the human *SLC24A4, SLC24A5*, and *Drosophila Nckx-x (Zydeco) genes* that have been associated with AI, OCA6, and seizures.

Experimental Procedures

Unless stated otherwise, all chemicals were purchased from Sigma and all tissue culture supplies were purchased from ThermoFisher Scientific.

pcDNA Preparation of the Mutant NCKX4 Proteins—The NCKX4 cDNA used in our study (accession number AF520705) was modified by introducing the Myc tag (EQKLISEEDL) into the extracellular loop (after amino acid 56 and includes Asp^{57} of the WT sequence) that precedes TMS1 to allow for easy detection of the expressed NCKX4 protein by Western blotting. The seven mutations in the NCKX4 protein summarized in Table 1 were prepared using the site-directed mutagenesis PCR technique; briefly, primers that included specific point mutations for the seven amino acid substitutions (G141S, A142T, A146E, A146V, S213R, L436R, and S499C) were prepared (Table 2) and used for the PCR. Q5 Master Mix (New England Biolabs, catalog number M0494S) was used to amplify DNA fragments containing the mutations. The PCR product was subcloned into pcDNA3.1 flanked by the ApaI and BamHI restriction sites. All products were sequenced to verify that the correct mutation was introduced (University of Calgary Sequencing Facility).

TABLE 1
Summary of mutations in NCKX genes and their associated genetic diseases

Mutation	Gene	NCKX isoform	Mutation in NCKX4 protein	Genetic disease	Ref.
G79S		*Drosophila*	G141S	Seizures	22
A80T		*Drosophila*	A142T	Seizures	22
A115E	c.344C>A	NCKX5	A146E	Non-syndromic oculocutaneous albinisim (ORCA6)	20
R174K	c.521G>A	NCKX5	R205K	Non-syndromic oculocutaneous albinisim (ORCA6)	21
S182R	c.546T>A	NCKX5	S213R	Non-syndromic oculocutaneous albinisim (ORCA6)	21
A146V	c.437C>T	NCKX4	A146V	Amelogenesis Imperfecta	4
L436R	c.1317T>G	NCKX4	L436R	Amelogenesis Imperfecta	11
S499C	c.1495A>T	NCKX4	S499C	Amelogenesis Imperfecta	12
Arg^{399} [a]	c.1015C>T	NCKX4		Amelogenesis Imperfecta	12
Chromosomal deletion	Chr14:680–722del	NCKX4		Amelogenesis Imperfecta	13

[a] Indicates a stop codon.

TABLE 2
Summary of NCKX4 mutations and the primers used to synthesize them in pcDNA 3.1

Mutation	Gene	Mutation in NCKX4 protein	Primers
G79S	*SLC24A4*	G141S	**F:** 5′-AGATGTGGCTtcAGCCACCTTC-3′ **R:** 5′-TCGCTCAGATGGAGTCTC-3′
A80T	*SLC24A4*	A142T	**F:** 5′-TGTGGCTGGAaCCACCTTCAT-3′ **R:** 5′-TCTTCGCTCAGATGGAGTC-3′
A115E	*SLC24A4*	A146E	**F:** 5′-GGAGCCACCTTCATGGagGCAGGAAGC-3′ **R:** 5′-TTGTTCCGTCTCTAGAGAAGATCTGTGAGAGACTCCATCTGAGC GAAGATGTGGCT-3′
R174K	*SLC24A4*	R205K	**F:** 5′-GTGGTGGGCCGTGTGCaagGACTCCGTGTACTACAC-3′ **R:** 5′-GTGTAGTACACGGAGTCCTTGCACACGGCCCACCAC-3′
S182R	*SLC24A4*	S213R	**F:** 5′-CTACACCATCcgTGTCATCGTGCTCATC-3′ **R:** 5′-TACACGGAGTCTCGGCA-3′
A146V	*SLC24A4*	A146V	**F:** 5′-ACCTTCATGGtTGCAGGAAGC-3′ **R:** 5′-GGCTCCAGCCACATCTTC-3′
L436R	*SLC24A4*	L436R	**F:** 5′-GGCCCCTCATCTTCCgCCTGTGCGTCACCAT-3′ **R:** 5′-ATGGTGACGCACAGGcGGAAGATGAGGGGCC-3′
S499C	*SLC24A4*	S499C	**F:** 5′-AGCAGGGACAtGTGTTCCAGAC-3′ **R:** 5′-GCCAGGAAAGTAATGCCC-3′

Plasmids were transformed into competent *Escherichia coli* cells and cells were grown overnight on LB agar plates. Colonies were picked the next day and cultured overnight in LB media at 37 °C with shaking. Plasmid DNA was purified using the Qiagen Endofree Maxi Kit (Qiagen, catalog number 12362).

Subculturing and Transient Transfection of HEK Cells—Human embryonic kidney cells (HEK293) were subcultured in DMEM and cells were split to 500,000 cells in 10-cm plates and left to grow overnight. Transient transfection of the different subcloned cDNAs in pcDNA3.1 (Invitrogen) was carried out with the Ca^{2+}-phosphate precipitation method as described before (34). The cells were harvested for experiments 48 h post-transfection using trypsin-EDTA. The transfection efficiency was 60–80%.

Transport Activity of the Mutant NCKX4 Proteins—NCKX transport assays were carried out after loading Na^+-enriched HEK293 cells expressing the mutant NCKX4 proteins with the Ca^{2+}-indicating dye Fluo4FF as described in detail elsewhere (28). HEK293 cells were enriched in internal Na^+ by carrying out the dye loading step in the presence of 500 μM of the Na^+/K^+-ATPase inhibitor ouabain. Briefly, the initial rates of K^+- and Ca^{2+}-induced rises in fluorescence due to Ca^{2+} influx via reverse Na^+/Ca^{2+}-K^+ exchange were measured in a cuvette containing $\sim 10^5$ of the Fluo4FF-loaded HEK293 cells. Further details are described in the legend of Fig. 3. Sigma plot 12.5 software was used to prepare Fig. 3 that illustrates Ca^{2+} transport activity of the WT and mutant NCKX4 proteins. These experiments were replicated 4 times and the linear rates of change in fluorescence observed within the first 5–30 s following the initiation of Ca^{2+} influx were calculated for both WT and mutant NCKX4 proteins to assess the relative activity of the latter compared with WT.

Surface Biotinylation and Western Blotting—HEK cells expressing the WT or mutant NCKX4 proteins were harvested 48 h post-transfection and surface biotinylation was carried out with 1 mM EZ-Link Sulfo-NHS-LC-Biotin (Pierce) as described (35). Briefly, 2.5 ml of 1 mM biotin solution was incubated with the re-suspended cell pellets for 10 min with gentle mixing. The reaction was terminated by adding 30 ml of 10 mM glycine solution. 1× PBS solution was used to wash the cells twice and the pellets were re-suspended in 1 ml of 1× PBS. The samples were then incubated with 0.0375% saponin for 1 min followed by another wash with PBS. After the washing steps, the cells were incubated in 150 μl of RIPA buffer on ice (20 mM Tris-HCl, pH 7.5, 150 mM NaCl, 1 mM Na_2EDTA, 1 mM EGTA, 1% Nonidet P-40, 1% sodium deoxycholate, 2.5 mM sodium pyrophosphate, 1 mM β-glycerophosphate, 1 mM Na_2VO_4, 1 μg/ml of leupeptin) plus 1 protease inhibitor tablet (Roche cOmplete Ultra, mini, EDTA-free easy pack per 10 ml of RIPA buffer) for 20 min. The supernatant was collected after centrifugation at 20,000 × *g* for 10 min. After the biotinylation reaction, 150 μg of total protein was added to 40 μl of streptavidin-agarose beads (ThermoFisher Scientific, catalog number S951) and 350 μl of TBS solution, and incubated overnight at 4 °C under continuous shaking. The beads were washed four times with a TBS-RIPA (7:1) solution and spun down at 1,000 × *g* for 5 min. After the washes, the beads were incubated with 20 μl of 200 mM acidic glycine solution (pH 2–3) and spun down at 1,000 × *g* for 5 min. The supernatants were neutralized with 5 μl of a 1 M Tris solution (pH 7.4) and mixed with 20 μl of 3× SDS sample buffer

(New England Biolabs). Proteins were separated on SDS-PAGE (4% stacking, 8.5% resolving) and Western blots were prepared for analysis on the LI-COR Odyssey two-channel IR Direct detection scanner as described before (28). Mouse Myc Ab (1:1,000 dilution, Cell Signaling Technologies, catalog number 2276) was used to develop the protein blot. The LI-COR Odyssey software was used to quantify total and surface protein levels from the Western blotting and biotinylation experiments.

Immunocytochemistry—48 h post-transfection, HEK293 cells were washed twice with PBS and then fixed for 10 min in 400 μl of 4% *p*-formaldehyde in PBS followed by another PBS wash. Cells on half of the plates were permeabilized with 500 μl of 0.2% Triton X-100 for 5 min, followed by three washes with PBS. The other half of the plates were kept in PBS and represent non-permeabilized cells. Cells on all plates were blocked with 400 μl of 10% horse serum (HS) in PBS for 1 h. After the blocking step, a quick wash was performed and cells were incubated with primary mouse Myc Ab (1:1000 dilution in 10% HS in PBS, Cell Signaling Technologies, catalog number 2276) and sheep TGN46-Ab (1:500 dilution in 10% HS in PBS, AbD Serotec, catalog number AHP500G) for 1 h. The cells were washed three times with PBS for 5 min and then incubated with the secondary Abs for 1 h in the dark (*e.g.* 500 μl of 2° goat anti-mouse Ab and goat anti-sheep Ab; 1:2000 dilution in 50% HS in PBS, Cell Signaling Technologies). Cell labeling was followed by four 5-min washes with PBS and a quick wash with deionized Millipore water. Excess water was wiped with Kim wipes and 8 μl of mounting media (ProLong AntiFade Reagent with DAPI, Vectashield Laboratories) was added to the plate. A coverslip was quickly placed on the top of the mounting media and the edges were sealed with clear nail polish to prevent dehydration. Finally, the plates were covered with parafilm and stored at 4 °C until used for imaging.

Fluorescence Imaging—Images were taken with the EVOS® FL Auto Imaging System. We used the single slider until the on-screen brightness of the signal was satisfactory and used this setting to capture images in high-quality mode. This represented a gain setting of 0 and an exposure time of 35–50 ms. Ten to 15 images were taken for WT and each mutant NCKX4 protein for the Triton (+T)-treated plates and 15–20 images for the untreated plates (−Triton). The experiment was replicated four times representing independent transfections and Fig. 5 illustrates representative images.

Data Analysis—The LI-COR Odyssey software was used to quantify total and surface protein levels from the Western blots and biotinylation experiments. Similarly, for the immunocytochemistry experiments, ImageJ was used to quantify the level of total and surface protein from images taken from HEK cells expressing either the WT or the mutant NCKX4 proteins. Briefly, these images were converted into gray scale, and a box was drawn around the labeled protein (whether on the surface or in the cytoplasm) to calculate pixel density in ImageJ. Similarly, using the Odyssey software, pixel density was calculated by drawing a box around the band and data are summarized in Fig. 6. The Student's *t* test was used to compare the mutant NCKX4 group to the wild-type NCKX4 group. A summary of the statistical analyses can be found in Fig. 6.

Results

Generation of NCKX4 Mutants—Several recent studies have linked mutations in the *SLC24A4* and *SLC24A5* genes to AI and OCA6, respectively. In addition, mutations in a *Drosophila* ortholog have been linked to an increased susceptibility to seizures. It is believed that all NCKXs share a common topology with 10 TMSs divided into two conserved clusters of five TMSs connected by a divergent cytoplasmic loop (Fig. 2*A*). Both TMSs clusters contain a highly conserved region (30–40 amino acids) referred to as the α-1 and α-2 repeats, respectively. The two α-repeats are thought to form the ion binding pocket and to coordinate ion transport via the alternating access model (Fig. 2*A*) (8). We used the human NCKX4 cDNA and introduced eight separate mutations leading to single residue substitutions in the NCKX4 protein that have been linked to the above mentioned diseases as detailed in Table 1. NCKX4 transfected into HEK293 cells yields strong functional protein activity allowing for high resolution activity measurements unlike the Nckx-x and NCKX5 clones. In the latter case, NCKX5 is not trafficked to the surface membrane but located in intracellular organelles preventing activity measurements of sufficient resolution (18, 27). The three *SLC24A5* mutations found in OCA6 patients concern residues highly conserved in the NCKX3–5 isoforms of humans as well as other species including zebrafish in which the role of NCKX5 was first elucidated (18). Fig. 2*B* shows the sequences of NCKX3, NCKX4, and NCKX5 and illustrates that all the mutations described concern residues conserved in the WT NCKX4 sequence except for the NCKX4 Leu^{436} residue, which has a leucine as well in NCKX5 but a valine residue in NCKX3.

Mutant NCKX4 Protein Transport Activity via Reverse Exchange—The mutant NCKX4 proteins were expressed in HEK293 cells. The transfected cells were loaded with the fluorescent Ca^{2+}-indicating dye Fluo4FF and NCKX-mediated Ca^{2+} influx via reverse exchange of wild-type and mutant NCKX4 proteins was measured as a rise of fluorescence as illustrated in Fig. 3. As we employed the low affinity Ca^{2+} indicating dye Fluo4FF (K_d = 9 μM), NCKX4-mediated Ca^{2+} influx rapidly increased the intracellular free [Ca^{2+}] to values in the 5–10 μM range (based on a typical transfection efficiency of 60–80%, data not illustrated). The WT NCKX4 activity traces are taken from three different experiments and in all cases paired with a mutant NCKX4 trace obtained from the same transfection experiment. In comparison with the WT NCKX4 protein activity, the G141S (8.5 ± 1.9%, n = 4) and A142T (22.7 ± 3%, n = 3) substitutions, representing the mutations found in the *Drosophila* NCKX-X, showed greatly diminished Ca^{2+} transport activity (in parentheses the percentage of WT NCKX4 activity). Similarly, the mutant NCKX4 protein carrying the R205K substitution, found in patients with OCA6 (21), showed a significant drop in transport activity (22.0 ± 3.3%, n = 6). In contrast, the other five substitutions (A146E, S213R, A146V, L436R, and S499C), representing mutations found in patients with AI or OCA6, resulted in mutant NCKX4 proteins with no measurable Ca^{2+} transport activity. This was also observed when we used Fluo4 as a Ca^{2+}-indicating dye, which has about a 20-fold higher affinity for Ca^{2+} compared with Fluo4FF, and would

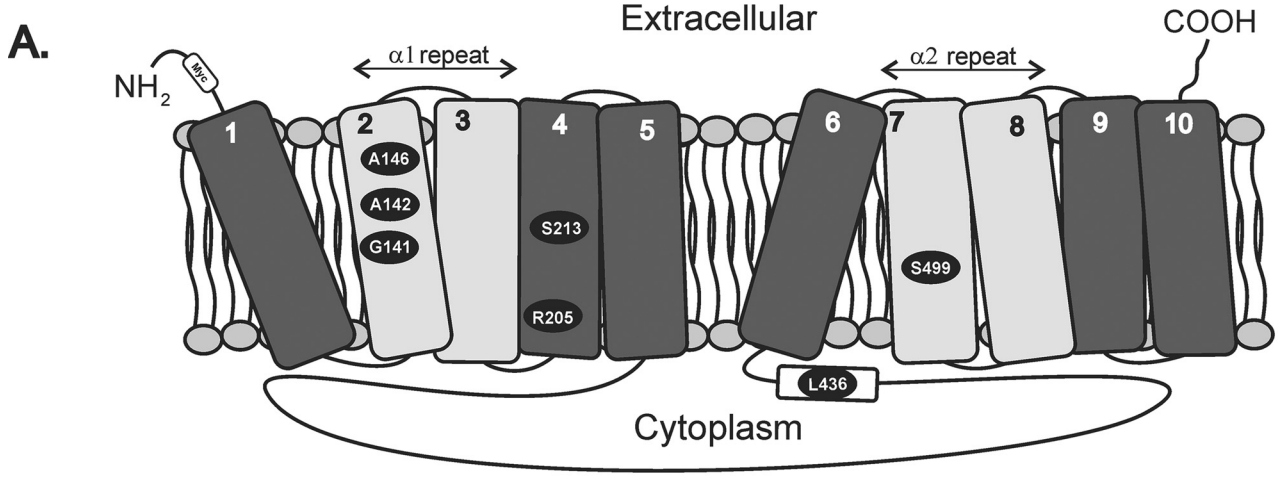

B.

```
hNCKX3   FYALAIVCDDFFVPSLEKICERLHLSEDVAGATFMAAGSSAPELFTSVIGVFITKGDVGV 180
hNCKX4   FYALAIVCDDFFVPSLEKICERLHLSEDVAGATFMAAGSSTPELFASVIGVFITHGDVGV 170
hNCKX5   FMAISIVCDEYFLPSLEIISESLGLSQDVAGTTFMAAGSSAPELVTAFLGVFITKGDIGI 139
         * *::****::*:**** *.* * **:***.*:***.****:***.::.:*****:**:*:

hNCKX3   GTIVGSAVFNILCIIGVCGLFAGQVVALSSWCLLRDSIYYTLSVIALIVFIYDEKVSWWE 240
hNCKX4   GTIVGSAVFNILCIIGVCGLFAGQVVRLTWWAVCRDSVYYTISVIVLIVFIYDEQIVWWE 230
hNCKX5   STILGSAIYNLLGICAACGLLSNTVSTLSCWPLFRDCAAYTISAAAVLGIIYDNQVYWYE 199
         .**:***::*:* * ..***::. *  *: * : *.  **:*. .:: :***::: *:*

hNCKX3   DEEEEEDEDDDEGPYTPFDTPSGKLETVKWAFTWPLSFVLYFTVPNCNKPRWEKWFMVTF 480
hNCKX4   QPPPPEPEPVEADFLSPFSVPEARGDKVKWVFTWPLIFLLCVTIPNCSKPRWEKFFMVTF 456
hNCKX5   -----------EDPPSVFNMPEADLKRIFWVLSLPIITLLFLTTPDCRKKFWKNYFVITF 338
                  .  : *. *..  . : *.:: *:  :* .* *:* *  *:::*::**

hNCKX3   ASSTLWIAAFSYMMVWMVTIIGYTLGIPDVIMGITFLAAGTSVPDCMASLIVARQGMGDM 540
hNCKX4   ITATLWIAVFSYIMVWLVTIIGYTLGIPDVIMGITFLAAGTSVPDCMASLIVARQGLGDM 517
hNCKX5   FMSAIWISAFTYILVWMVTITGETLEIPDTVMGLTLLAAGTSIPDTIASVLVARKGKGDM 398
           :::**:.*:*::**:*** * ** ***.:**:*:*****:** :**::***:* ***
```

FIGURE 2. **Schematic representation of the current topological model of the human NCKX and the sequence alignment of NCKX3, −4, and −5.** *Panel A* shows the NCKX topological model that consists of two sets of 5 TMS separated by a large cytoplasmic loop. TMS 2–3 and TMS 7–8 (highlighted in *light gray*) contain highly conserved regions known as the α1 and α2 repeats. The highlighted residues represent those that have been linked to genetic diseases as summarized in Table 1. *Panel B* shows the alignment of the NCKX3, –4, and –5 sequences with the residues linked to genetic diseases in *bold*. The sequence alignment was prepared using ClustalW2. An *asterisk* (*) denotes conserved residues, a *colon* (:) denotes conserved substitutions, and a *period* (.) denotes semi-conserved substitutions, *i.e.* amino acids side chains share similar shapes.

allow us to detect very low mutant NCKX4 activity under conditions wherein WT NCKX4 activity quickly results in dye saturation (using the two dyes we could reliably detect mutant NCKX4 activity as low as 1% of WT activity). Finally, we examined the effect of WT NCKX4 protein expression (by lowering the amount of DNA used during the transfection) on NCKX4 transport activity; lowering the DNA concentration by 15-fold greatly lowered functional expression but transport activity could clearly be detected even though NCKX4 protein expression was nearly undetectable (see Fig. 4).

Mutant NCKX4 Protein Expression—Lack of transport activity or reduced transport activity of the mutant NCKX4 proteins was not associated with changes in total protein expression levels as judged by Western blotting analysis using the Myc tag inserted in our NCKX4 cDNAs (Fig. 4*A*). The Western blot invariably showed a three band pattern for WT NCKX4 and all mutant NCKX4 proteins. The two lower bands likely represented full-length NCKX4 protein and NCKX4 protein from which the signal peptide has been cleaved. This is consistent with what was reported previously for NCKX2 expressed in cell

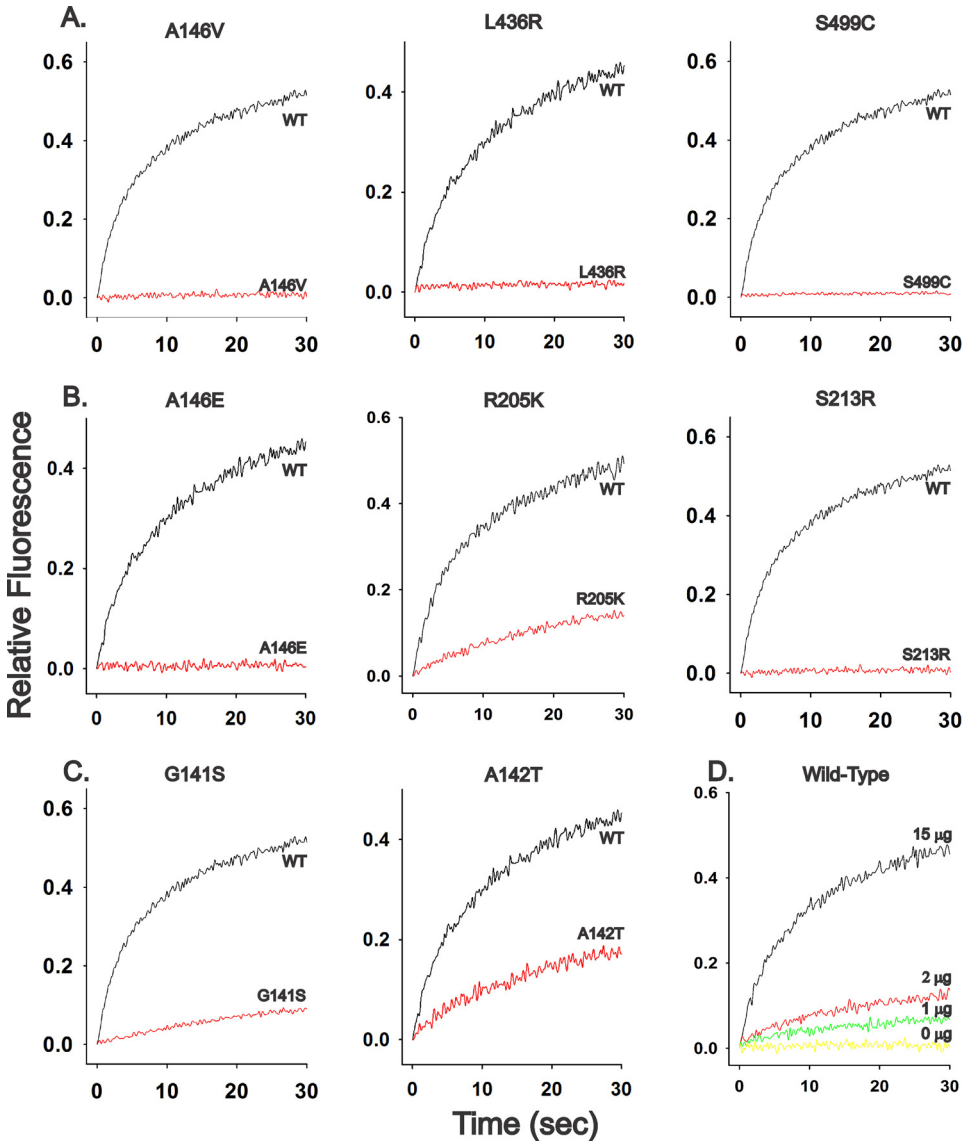

FIGURE 3. **Changes in free $[Ca^{2+}]_i$ mediated by WT and mutant NCKX4 proteins measured with Fluo4FF.** HEK293 cells expressing WT or one of the eight NCKX mutant proteins were loaded with Fluo4FF and Na^+ as described before (28). 50 μl of the concentrated suspension of Fluo4FF-loaded HEK293 cells were diluted under constant stirring in a cuvette containing 1.95 ml of 150 mM LiCl, 20 mM HEPES (adjusted to pH 7.4 with arginine), 50 mM KCl, and 0.1 mM EDTA. NCKX-mediated Ca^{2+} influx was initiated at time 0 by addition of 0.35 mM $CaCl_2$ resulting in a steady rise in Fluo4FF fluorescence but only when cells expressed a functionally competent NCKX4. The *ordinate* indicates fluorescence normalized to the maximal fluorescence obtained when the cells were permeabilized with saponin in the presence of a saturating concentration of 5 mM $CaCl_2$. *Panel A* shows NCKX mutants associated with AI; *panel B* shows NCKX4 mutants associated with non-syndromic OCA; *panel C* shows NCKX mutants linked to increased propensity for seizures in *Drosophila*, and *panel D* illustrates the effect of different DNA concentrations during the transfection on WT NCKX4 expression as judged by different rates of Ca^{2+} transport.

lines (36). The high molecular weight band may represent an NCKX4 dimer as NCKX1 and NCKX2 have been shown to form dimers when expressed in cell lines; moreover, cysteine-based cross-linking resulted in NCKX2 dimers of strikingly different molecular weights dependent on the location of the cysteine residue used for the cross-linking and this could account for the anomalously high M_r seen here for the putative NCKX4 dimer (37). For most mutant NCKX4 proteins expression levels were not statistically significant different from WT NCKX4, but the mutant NCKX4 proteins carrying the A142T and S213R substitutions appeared to result in slightly higher protein expressions levels compared with WT NCKX4 expression (Fig. 6*A*, p value <0.05).

Surface NCKX4 Expression as Assessed by Surface Biotinylation and Immunocytochemistry—Although mutant NCKX4 protein levels were not reduced in our HEK293 cell expression experiments, lack of transport activity could also reflect a surface membrane trafficking defect rather than a functionally inactive exchanger. We used both surface biotinylation and immunocytochemistry to address this question. The R205K mutation (21) was reported after all the work on the other mutants had been completed. For this mutant NCKX4 protein, we only carried out the immunohistochemistry experiment as this represents the more direct method of surface localization.

Biotinylation of surface proteins was carried out with the membrane-impermeant reagent EZ-Link Sulfo-NHS-LC-Bio-

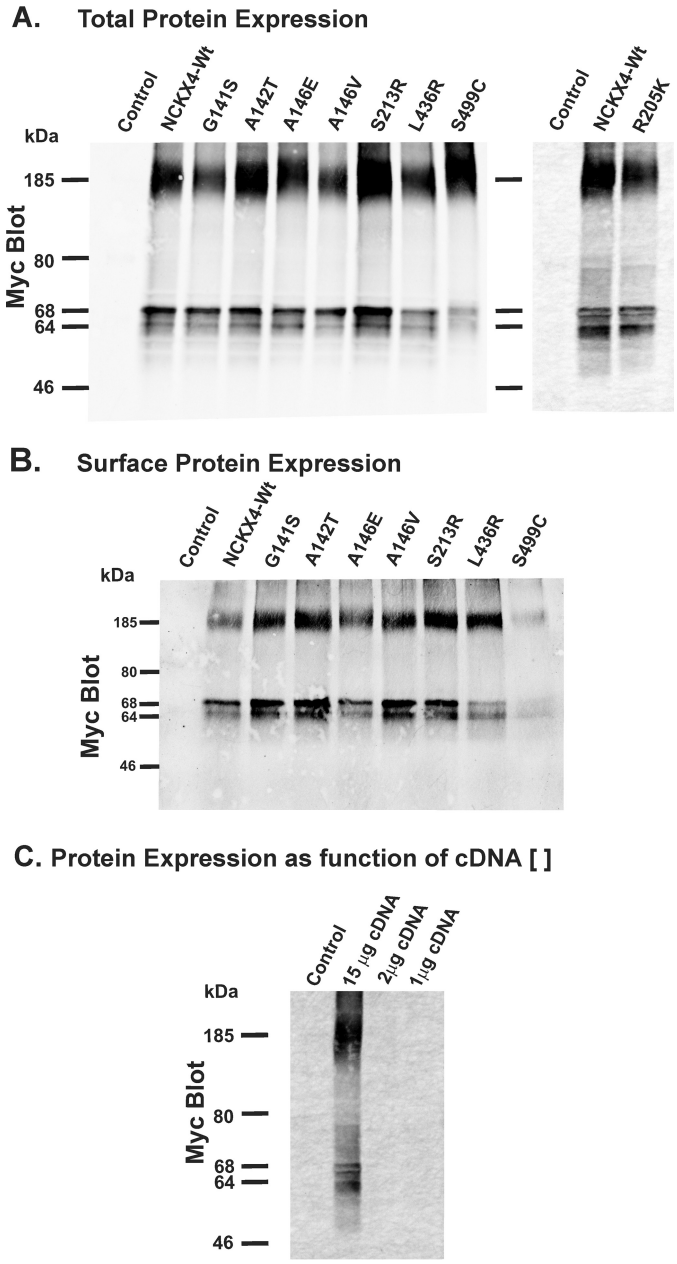

FIGURE 4. **Protein expression of WT and mutant NCKX4 proteins in HEK293 cells.** Western blots are shown of the Myc-tagged WT and mutant NCKX4 proteins expressed in HEK293 cells. *Panel A* represents lanes loaded with 20 μg of total cell protein of HEK cells expressing the indicated WT and mutant NCKX4 proteins. *Panel B* represents surface expression of the biotinylated and Myc-tagged WT and mutant NCKX4 proteins as described under "Experimental Procedures." *Panel C* shows WT NCKX4 expression as a function of the amount of DNA used during the transfection. The blots were developed with the Myc tag (9B11) mouse monoclonal primary antibody and the goat anti-mouse IRDye 800CW secondary antibody. The blots were scanned with the LI-COR Odyssey two-channel IR Direct detection scanner.

tin in intact HEK293 cells expressing the mutant or WT NCKX4. The biotinylated surface NCKX4 proteins were purified as described under "Experimental Procedures." The Myc blot of the surface WT and mutant NCKX4 proteins is shown in Fig. 4*B*, and, with the exception of the S499C mutant, the amount of surface mutant NCKX4 protein was not different from that observed for the WT NCKX4 (Fig. 6*B*). From the data shown in Fig. 4 we conclude that, with exception of the S499C mutant, neither reduced protein expression levels nor diminished trafficking to the plasma membrane were major contributors to the reduction or abolition of transport observed for the mutant NCKX4 proteins (Fig. 3).

We used immunocytochemistry to visualize the location of the WT and mutant NCKX4 proteins in HEK293 cells (Fig. 5). When comparing images obtained for permeabilized with those of non-permeabilized cells, it is evident that most of the expressed WT or mutant NCKX4 protein was localized within the HEK293 cells rather than on the cell surface (note that the Myc tag is located in the extracellular N-terminal loop of NCKX4, Fig. 2*A*) and this is likely a consequence of using an overexpression system. Nevertheless, surface expression was readily observed and accounted for the robust NCKX4 transport activity observed (Fig. 3). Consistent with the surface biotinylation results (Fig. 4*B*), surface membrane expression was detected for all the NCKX4 mutants with the exception of the S499C mutant. Total protein expression examined in a large number of cells was very similar for WT NCKX4 and all mutant NCKX4 including the S499C mutant (Fig. 6*C*). Analyzing a large number of cells also revealed very similar surface protein expression for WT and all mutant NCKX4 proteins (Fig. 6*D*) with the exception of the S499C mutant NCKX4 protein for which surface localization was never observed. As these are single cell measurements a wide range of expression levels was observed, in particular with a few cells expressing a very large amount of (mutant) NCKX4 protein. No difference in total protein expression levels was found as judged by analyzing the permeabilized cells and this includes the S499C mutant Fig. 6*C*).

Discussion

In this study we have examined functional consequences of mutations in the *SLC24A4* and *SLC24A5* genes that have been reported for patients with AI (4, 11–13) and OCA (20), respectively. Five of the six mutations resulted in single residue substitutions in the mutant NCKX4 proteins that had no measurable functional activity in our transport assay, whereas in one case the mutant NCKX4 protein showed strongly reduced transport function (Fig. 3). For five of the mutant NCKX4 proteins, abolition or reduction of transport activity was not caused by a reduction in protein expression or by impaired trafficking to the surface membrane (Figs. 4 and 5). In one case (S499C) protein expression was not reduced but little or no protein was found on the plasma membrane (Figs. 5 and 6). We have previously reported on the homologous substitution (S545C) in the human NCKX2 protein expressed in insect High Five cells (35) and HEK293 cells (34, 38) and observed greatly reduced but measurable Ca^{2+} transport activity. This is consistent with our observation on the NCKX4 S499C mutant, although, unlike the S499C NCKX4 mutant, some surface membrane localization and transport activity was observed for the homologous S545C NCKX2 mutant. The NCKX2 Ser^{545}/NCKX4 Ser^{499} residue is highly conserved in both eukaryotic NCX and NCKX proteins as well as in prokaryotic NCX proteins, and the S545A substitution in NCKX2 was found to result in a large decrease in Na^+ affinity (39). In the crystal structure of the archaebacterial NCX_Mj Na^+/Ca^{2+} exchanger the homologous Ser^{210} residue

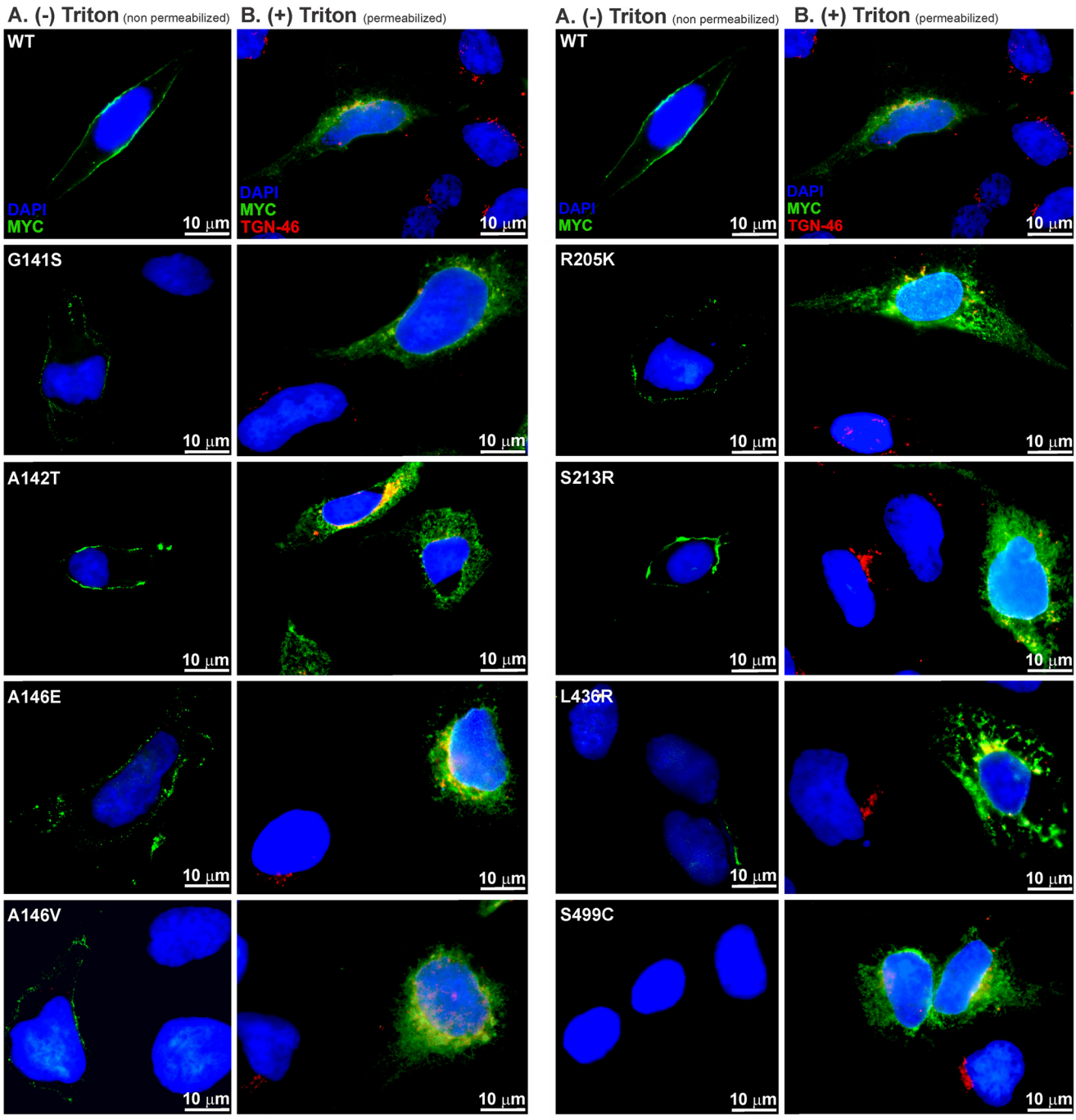

FIGURE 5. **Surface expression of WT and mutant NCKX4 in HEK293.** *Panel A* (*No Triton*), non-permeabilized cells show Ab labeling of Myc-tagged WT and mutant NCKX4 (*green*) that appears to be restricted to the plasma membrane only. Labeling with Ab against the trans-Golgi network marker TGN46 (*red*) was used as a control for the absence of permeabilized or leaky cells. *Panel B* (*With Triton*), cells permeabilized with 0.2% Triton X-100 show large amounts of expressed NCKX4 protein present in intracellular organelles, clearly distinct from the much more restricted pattern observed in intact cells illustrated in *panel A*. Unlike in intact cells, trans-Golgi network (*TGN*) staining (*red*) was detected in all permeabilized cells. Sheep anti-TGN46 and mouse anti-Myc were used to label TGN46 (*red*) and Myc-tagged NCKX4 (*green*), respectively. Representative images are shown for each mutant representing four independent transfection experiments.

is one of the Na^+ coordinating residues consistent with its critical role in NCX/NCKX transport activity (40). The other four non-functional AI and OCA6 mutants concerned highly conserved residues but only two (A146V and A146E) targeted a residue that is part of the α-repeats. We have previously examined the homologous A181S and A181C substitutions in NCKX2 and found both to have WT activity (35). The deleterious effect of the A146E substitution is not unexpected as it introduces an additional hydrophilic and charged residue in TMS2, but abolition of activity caused by the conservative A146V was surprising as the less conservative A181S and A181C substitutions resulted in mutant NCKX2 proteins with WT activity (35). Therefore, we introduced the same substitution in the NCKX2 and NCKX3 proteins and observed a complete abolition of transport activity (data not shown), consistent with the effect of the A146V substitution in NCKX4 (Fig. 3).

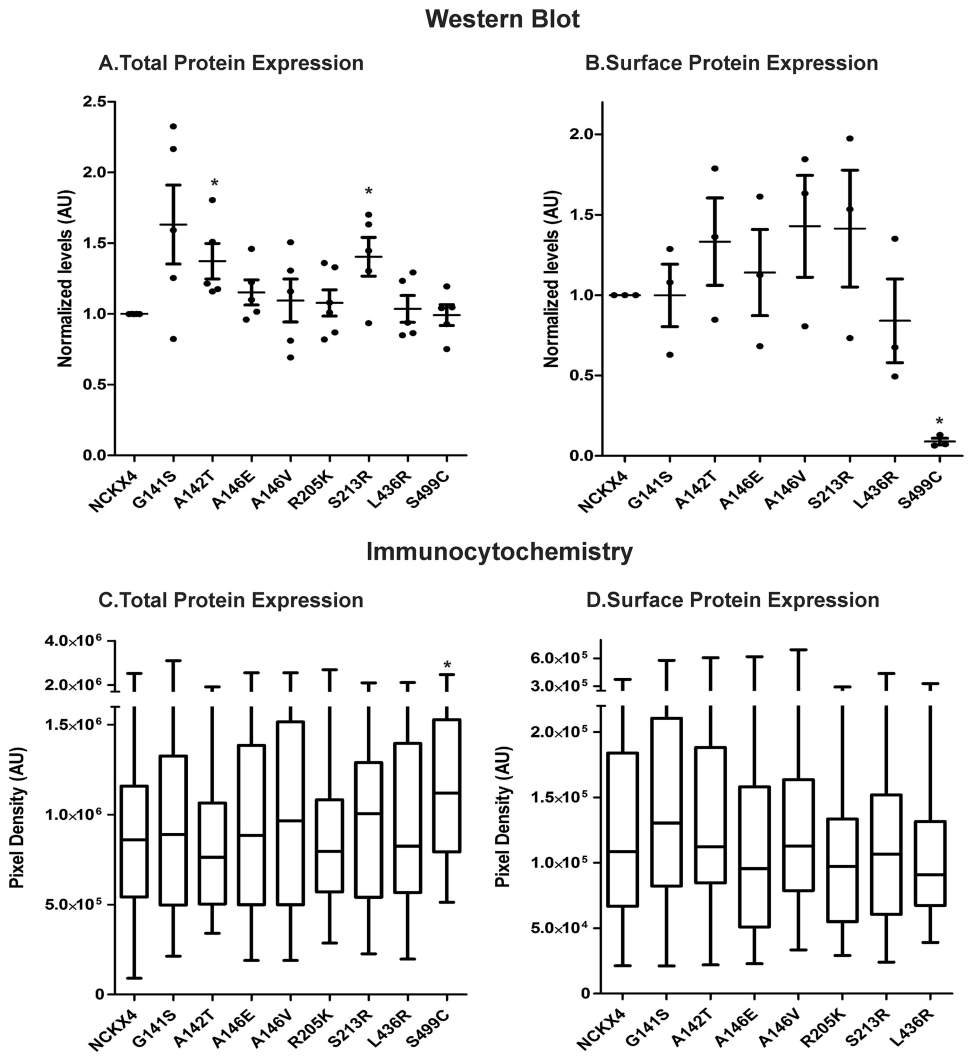

FIGURE 6. **Total and surface NCKX4 protein expression levels using Western blot, surface biotinylation, and immunocytochemistry experiments.** *Panel A* presents total NCKX4 mutant protein levels normalized to WT NCKX4 taken from Western blots loaded with 20 μg of total protein. Data points from five different transfection experiments are shown with the average ± S.E. No significant reductions were observed but significant increases in protein levels were detected for the A142T and S213R substitutions ($p < 0.05$ for both, presented with an *asterisk*). *Panel B* presents surface mutant NCKX4 protein levels normalized to WT NCKX4; data points present surface protein levels (with average value ± S.E.) obtained from three surface biotinylation experiments representing separate transfections and using 150 μg of total protein. No significant differences were observed except for the lack of surface presence of the S499C substitution ($p < 0.0001$, presented with an *asterisk*). *Panel C* illustrates the total protein levels of WT and mutant NCKX4 measured as pixel density from the immunocytochemistry experiments as described under "Experimental Procedures" and represented in a box and whisker plot. The *box* represents the pixel density observed in 25–75% of the population of cells, whereas the extensions indicate the minimum and maximum values obtained. At least 30 cells were measured representing three different transfection experiments. No significant reductions were observed but a significant increase in protein levels was detected for the S499C substitution ($p < 0.05$, presented with an *asterisk*). *Panel D* illustrates surface protein levels of WT and mutant NCKX4 measured as pixel density from the immunocytochemistry experiments as described under "Experimental Procedures" and represented in a box and whisker plot. The *box* represent the pixel density observed in 25–75% of the population of cells, whereas the extensions indicate the minimum and maximum values obtained. At least 30 cells were measured representing three different transfection experiments. No surface labeling was ever observed for HEK cells transfected with the NCKX4 S499C substitution.

Like the Ser^{545} residue, discussed above, the Ala^{181} residue is highly conserved in eukaryotic NCX and NCKX proteins and it is also conserved in the archeabacterial Na^+/Ca^{2+} exchanger NCX_Mj for which a crystal structure was obtained recently (40). In this structure the homologous Ala^{47} residue is thought to be a coordinating residue for one of the Na^+ ions.

The other two transport abolishing mutations, resulting in the S213R and L436R substitutions, as well as the R205K substitution that resulted in a 78% reduction in transport rate, involved residues that have not been reported before in other NCKX isoforms. The S213R OCA6 mutation introduced a positive charge within TMS 4, which might be deleterious for a protein that operates as a cation exchanger. The AI L436R mutation presented perhaps the most unexpected case as it is not located in the two sets of 5 TMS but in a hydrophobic segment at the end of the large cytosolic loop, just in front of TMS6. In our laboratory we have mutated more than 150 residues in the NCKX2 protein sequence and found that complete abolition of transport function was a rather rare occurrence. Finally, the R205K substitution is surprising as it represents a rather conservative change; we have examined the less conservative R205A substitution in NCKX2 and observed a complete abolition of transport (data not illustrated). Taken together, we believe that it is highly significant that all six mutations found in

patients with AI and OCA6 resulted in mutant NCKX4 proteins that showed a large reduction to a complete abolition of cation transport when expressed in HEK293 cells despite the fact that we are able to detect functional activity as low as 1% of that of WT NCKX4. Thus, we believe our data are strongly supportive of the genetic studies describing these mutations. It is important to reiterate here that we used NCKX4 mutant proteins carrying the *SLC24A5* mutations due to the lack of a sufficiently sensitive assay for the function of NCKX5 proteins located in internal organelles. Nevertheless, as these residues are highly conserved between the NCKX1–3 isoforms of humans and other species, we believe that these substitutions when introduced in NCKX5 would also result in a loss of transport function. The two mutations in the *Drosophila Nckx-x* gene that resulted in an increased susceptibility to seizures (22) are part of the first α-repeat and substitutions of the homologous residues that have been studied before in NCKX2. The homologous substitutions to G141A and G141C, *i.e.* G176A and G176C, resulted in mutant NCKX2 proteins with greatly reduced but measurable functional activity (<10% of WT activity) (35, 39). With respect to the NCKX4 A142T substitution, the homologous A111T substitution in both alleles of the human *SLC24A5* gene was shown to be a major determinant of light skin in people from European descent (18, 19). The homologous A177T substitution in NCKX2 reduced activity to ~25% of WT NCKX2 activity (27), consistent with the reduction of the A142T NCKX4 mutant reported here (~23% of WT NCKX4). The *Drosophila* NCKX-X is known to be related to the human NCKX3 and NCKX4 proteins and it will be interesting to examine whether mutations in the *SLC24A3* and/or *SLC24A4* genes have a similar effect in humans as well.

In conclusion, the significant drop or complete abolition of function in NCKX proteins that carry one of the mutations in the *SLC24A* genes that have been associated with AI and OCA6 strongly support the genetic studies describing these mutations. The data presented here also illustrate that the phenotype observed is due to a defect in transport activity.

Author Contributions—P. P. M. S., A. H. J., and R. T. S. designed the study. A. H. J. performed the mutations in pcDNA and tested the function of the mutant proteins expressed in HEK cells (presented in Fig. 3). A. H. J. performed the surface biotinylation experiments (presented in Fig. 4). A. H. J. and T. P. R. performed the immunocytochemistry experiments and prepared Fig. 5. R. T. S. and A. H. J. performed the Western bloting analysis and prepared Fig. 3. A. H. J. prepared the rest of the figures and tables. P. P. M. S. and A. H. J. gathered all the data and wrote the manuscript. All authors analyzed the results, reviewed and approved the final version of the manuscript.

Acknowledgment—We thank Dr. Frank Visser (Hotchkiss Brain Institute Molecular Core Facility, University of Calgary) for help with the preparation of some of the mutant NCKX proteins.

References

1. Hubbard, M. J. (1995) Calbindin28kDa and calmodulin are hyperabundant in rat dental enamel cells. Identification of the protein phosphatase calcineurin as a principal calmodulin target and of a secretion-related role for calbindin28kDa. *Eur. J. Biochem.* **230,** 68–79
2. Hubbard, M. J. (2000) Calcium transport across the dental enamel epithelium. *Crit. Rev. Oral Biol. Med.* **11,** 437–466
3. Splawski, I., Timothy, K. W., Sharpe, L. M., Decher, N., Kumar, P., Bloise, R., Napolitano, C., Schwartz, P. J., Joseph, R. M., Condouris, K., Tager-Flusberg, H., Priori, S. G., Sanguinetti, M. C., and Keating, M. T. (2004) $Ca_V1.2$ calcium channel dysfunction causes a multisystem disorder including arrhythmia and autism. *Cell* **119,** 19–31
4. Wang, S., Choi, M., Richardson, A. S., Reid, B. M., Seymen, F., Yildirim, M., Tuna, E., Gençay, K., Simmer, J. P., and Hu, J. C. (2014) STIM1 and SLC24A4 are critical for enamel maturation. *J. Dent. Res.* **93,** 94S-100S
5. Picard, C., McCarl, C. A., Papolos, A., Khalil, S., Lüthy, K., Hivroz, C., LeDeist, F., Rieux-Laucat, F., Rechavi, G., Rao, A., Fischer, A., and Feske, S. (2009) STIM1 mutation associated with a syndrome of immunodeficiency and autoimmunity. *N. Engl. J. Med.* **360,** 1971–1980
6. Lacruz, R. S., Smith, C. E., Kurtz, I., Hubbard, M. J., and Paine, M. L. (2013) New paradigms on the transport functions of maturation-stage ameloblasts. *J. Dent. Res.* **92,** 122–129
7. Lytton, J. (2007) Na^+/Ca^{2+} exchangers: three mammalian gene families control Ca^{2+} transport. *Biochem. J.* **406,** 365–382
8. Schnetkamp, P. P. (2013) The SLC24 gene family of Na^+/Ca^{2+}-K^+ exchangers: from sight and smell to memory consolidation and skin pigmentation. *Mol. Aspects Med.* **34,** 455–464
9. Okumura, R., Shibukawa, Y., Muramatsu, T., Hashimoto, S., Nakagawa, K., Tazaki, M., and Shimono, M. (2010) Sodium-calcium exchangers in rat ameloblasts. *J. Pharmacol. Sci.* **112,** 223–230
10. Hu, P., Lacruz, R. S., Smith, C. E., Smith, S. M., Kurtz, I., and Paine, M. L. (2012) Expression of the sodium/calcium/potassium exchanger, NCKX4, in ameloblasts. *Cells Tissues Organs* **196,** 501–509
11. Herzog, C. R., Reid, B. M., Seymen, F., Koruyucu, M., Tuna, E. B., Simmer, J. P., and Hu, J. C. (2015) Hypomaturation amelogenesis imperfecta caused by a novel SLC24A4 mutation. *Oral Surg. Oral Med. Oral Pathol. Oral Radiol.* **119,** e77–81
12. Parry, D. A., Poulter, J. A., Logan, C. V., Brookes, S. J., Jafri, H., Ferguson, C. H., Anwari, B. M., Rashid, Y., Zhao, H., Johnson, C. A., Inglehearn, C. F., and Mighell, A. J. (2013) Identification of mutations in SLC24A4, encoding a potassium-dependent sodium/calcium exchanger, as a cause of amelogenesis imperfecta. *Am. J. Hum. Genet.* **92,** 307–312
13. Seymen, F., Lee, K. E., Tran Le, C. G., Yildirim, M., Gencay, K., Lee, Z. H., and Kim, J. W. (2014) Exonal deletion of SLC24A4 causes hypomaturation amelogenesis imperfecta. *J. Dent. Res.* **93,** 366–370
14. Stephan, A. B., Tobochnik, S., Dibattista, M., Wall, C. M., Reisert, J., and Zhao, H. (2012) The Na^+/Ca^{2+} exchanger NCKX4 governs termination and adaptation of the mammalian olfactory response. *Nat. Neurosci.* **15,** 131–137
15. Li, X. F., and Lytton, J. (2014) An essential role for the K+-dependent Na^+/Ca^{2+}-exchanger, NCKX4, in melanocortin-4-receptor-dependent satiety. *J. Biol. Chem.* **289,** 25445–25459
16. Sulem, P., Gudbjartsson, D. F., Stacey, S. N., Helgason, A., Rafnar, T., Magnusson, K. P., Manolescu, A., Karason, A., Pálsson, A., Thorleifsson, G., Jakobsdottir, M., Steinberg, S., Palsson, S., Jonasson, F., Sigurgeirsson, B., *et al.* (2007) Genetic determinants of hair, eye and skin pigmentation in Europeans. *Nat. Genet.* **39,** 1443–1452
17. Pośpiech, E., Draus-Barini, J., Kupiec, T., Wojas-Pelc, A., and Branicki, W. (2011) Gene-gene interactions contribute to eye colour variation in humans. *J. Hum. Genet.* **56,** 447–455
18. Lamason, R. L., Mohideen, M. A., Mest, J. R., Wong, A. C., Norton, H. L., Aros, M. C., Jurynec, M. J., Mao, X., Humphreville, V. R., Humbert, J. E., Sinha, S., Moore, J. L., Jagadeeswaran, P., Zhao, W., Ning, G., *et al.* (2005) SLC24A5, a putative cation exchanger, affects pigmentation in zebrafish and humans. *Science* **310,** 1782–1786
19. Stokowski, R. P., Pant, P. V., Dadd, T., Fereday, A., Hinds, D. A., Jarman, C., Filsell, W., Ginger, R. S., Green, M. R., van der Ouderaa, F. J., and Cox, D. R. (2007) A genomewide association study of skin pigmentation in a South Asian population. *Am. J. Hum. Genet.* **81,** 1119–1132
20. Morice-Picard, F., Lasseaux, E., François, S., Simon, D., Rooryck, C., Bieth, E., Colin, E., Bonneau, D., Journel, H., Walraedt, S., Leroy, B. P., Meire, F., Lacombe, D., and Arveiler, B. (2014) SLC24A5 mutations are associated with non-syndromic oculocutaneous albinism. *J. Investig. Dermatol.* **134,** 568–571

21. Bertolotti, A., Lasseaux, E., Plaisant, C., Trimouille, A., Morice-Picard, F., Rooryck, C., Lacombe, D., Couppie, P., and Arveiler, B. (2016) Identification of a homozygous mutation of SLC24A5 (OCA6) in two patients with oculocutaneous albinism from French Guiana. *Pigment Cell Melanoma Res.* **29,** 104–106
22. Melom, J. E., and Littleton, J. T. (2013) Mutation of a NCKX eliminates glial microdomain calcium oscillations and enhances seizure susceptibility. *J. Neurosci.* **33,** 1169–1178
23. Schnetkamp, P. P., Jalloul, A. H., Liu, G., and Szerencsei, R. T. (2014) The SLC24 family of K^+-dependent Na^+-Ca^{2+} exchangers: structure-function relationships. *Curr. Top. Membr.* **73,** 263–287
24. Winkfein, R. J., Pearson, B., Ward, R., Szerencsei, R. T., Colley, N. J., and Schnetkamp, P. P. (2004) Molecular characterization, functional expression and tissue distribution of a second NCKX Na^+/Ca^{2+}-K^+ exchanger from *Drosophila*. *Cell Calcium* **36,** 147–155
25. Li, X. F., Kraev, A. S., and Lytton, J. (2002) Molecular cloning of a fourth member of the potassium-dependent sodium-calcium exchanger gene family, NCKX4. *J. Biol. Chem.* **277,** 48410–48417
26. Chi, A., Valencia, J. C., Hu, Z. Z., Watabe, H., Yamaguchi, H., Mangini, N. J., Huang, H., Canfield, V. A., Cheng, K. C., Yang, F., Abe, R., Yamagishi, S., Shabanowitz, J., Hearing, V. J., Wu, C., Appella, E., and Hunt, D. F. (2006) Proteomic and bioinformatic characterization of the biogenesis and function of melanosomes. *J. Proteome Res.* **5,** 3135–3144
27. Ginger, R. S., Askew, S. E., Ogborne, R. M., Wilson, S., Ferdinando, D., Dadd, T., Smith, A. M., Kazi, S., Szerencsei, R. T., Winkfein, R. J., Schnetkamp, P. P., and Green, M. R. (2008) SLC24A5 encodes a trans-Golgi network protein with potassium-dependent sodium-calcium exchange activity that regulates human epidermal melanogenesis. *J. Biol. Chem.* **283,** 5486–5495
28. Jalloul, A. H., Szerencsei, R. T., and Schnetkamp, P. P. (2016) Cation dependencies and turnover rates of the human K^+-dependent Na^+-Ca^{2+} exchangers NCKX1, NCKX2, NCKX3 and NCKX4. *Cell Calcium* **59,** 1–11
29. Kinjo, T. G., Szerencsei, R. T., Winkfein, R. J., Kang, K.-J., and Schnetkamp, P. P. (2003) Topology of the retinal cone NCKX2 Na/Ca-K exchanger. *Biochemistry* **42,** 2485–2491
30. Szerencsei, R. T., Kinjo, T. G., and Schnetkamp, P. P. (2013) The topology of the C-terminal sections of the NCX1 Na^+ /Ca^{2+} exchanger and the NCKX2 Na^+/Ca^{2+}-K^+ exchanger. *Channels* **7,** 109–114
31. Schnetkamp, P. P. M., Basu, D. K., and Szerencsei, R. T. (1989) Na-Ca exchange in the outer segments of bovine rod photoreceptors requires and transports potassium. *Am. J. Physiol. Cell Physiol.* **257,** C153-C157
32. Dong, H., Light, P. E., French, R. J., and Lytton, J. (2001) Electrophysiological characterization and ionic stoichiometry of the rat brain K^+-dependent Na^+/Ca^{2+} exchanger, NCKX2. *J. Biol. Chem.* **276,** 25919–25928
33. Szerencsei, R. T., Prinsen, C. F., and Schnetkamp, P. P. (2001) The stoichiometry of the retinal cone Na/Ca-K exchanger heterologously expressed in insect cells: comparison with the bovine heart Na/Ca exchanger. *Biochemistry* **40,** 6009–6015
34. Kang, K.-J., Kinjo, T. G., Szerencsei, R. T., and Schnetkamp, P. P. (2005) Residues contributing to the Ca^{2+} and K^+ binding pocket of the NCKX2 Na^+/Ca^{2+}-K^+ exchanger. *J. Biol. Chem.* **280,** 6823–6833
35. Winkfein, R. J., Szerencsei, R. T., Kinjo, T. G., Kang, K.-J., Perizzolo, M., Eisner, L., and Schnetkamp, P. P. (2003) Scanning mutagenesis of the α repeats and of the transmembrane acidic residues of the human retinal cone Na/Ca-K exchanger. *Biochemistry* **42,** 543–552
36. Kang, K.-J., and Schnetkamp, P. P. (2003) Signal sequence cleavage and plasma membrane targeting of the rod NCKX1 and cone NCKX2 Na^+/Ca^{2+}-K^+ exchangers. *Biochemistry* **42,** 9438–9445
37. Kang, K.-J., Bauer, P. J., Kinjo, T. G., Szerencsei, R. T., Bonigk, W., Winkfein, R. J., and Schnetkamp, P. P. (2003) Assembly of Retinal Rod or Cone Na^+/Ca^{2+}-K^+ exchangers oligomers with cGMP-gated channel subunits as probed with heterologously expressed cDNAs. *Biochemistry* **42,** 4593–4600
38. Altimimi, H. F., and Schnetkamp, P. P. (2007) Na^+-dependent inactivation of the retinal cone/brain Na^+/Ca^{2+}-K^+ exchanger NCKX2. *J. Biol. Chem.* **282,** 3720–3729
39. Altimimi, H. F., Fung, E. H., Winkfein, R. J., and Schnetkamp, P. P. (2010) Residues contributing to the Na^+-binding pocket of the SLC24 Na^+/Ca^{2+}-K^+ exchanger NCKX2. *J. Biol. Chem.* **285,** 15245–15255
40. Liao, J., Li, H., Zeng, W., Sauer, D. B., Belmares, R., and Jiang, Y. (2012) Structural insight into the ion-exchange mechanism of the sodium/calcium exchanger. *Science* **335,** 686–690